Localization in Inconsistent WiFi Environments*

Hsin-Min Cheng and Dezhen Song

Abstract As WiFi becomes more and more popular, indoor environments are often covered with access points (APs) many of which are temporarily generated by mobile devices. On the other hand, more and more infrastructural APs are equipped with beamforming capabilities which adjust radiation patterns according to client locations. These APs have large variations of signal fields. The inconsistent WiFi environments present a challenge for localization tasks when the client cannot communicate with APs. Here we report a new algorithm targeted at handling inconsistent APs. We develop a windowed majority voting and statistical hypothesis testing-based approach to remove APs with large displacements between reference and query data sets. We then refine the localization by applying maximum likelihood estimation method to the closed-form posterior location distribution over the filtered signal strength and AP sets in the time window. We determine the time window length by minimizing Shannon entropy of the posterior location distribution. We have implemented our algorithm and our method outperforms its counterparts in physical experiments. Our method achieves a mean localization error of less than 3.7 meters even when 70% of APs are inconsistent.

1 Introduction

Indoor localization has become more important in recent years as mobile robots and mobile device users often need to find their locations where global positioning system (GPS) signals are unavailable. One low-cost solution is to utilize WiFi signals in the environment. The number of WiFi access points (APs) has dramatically increased in the past few years. A large number of APs are temporarily generated by cellphones and other mobile devices. Moreover, more and more infrastructural APs are equipped with beamforming capabilities which adjust radiation patterns according to client locations. These APs have large variation in their signal fields. We name those APs as inconsistent APs. Fig. 1 shows an example of a WiFi environment with inconsistent APs which dramatically change received signal strength

---

Department of Computer Science and Engineering, Texas A&M University, College Station, TX 77843, USA. Emails: e-mail: {hmcheng, dzsong}@cse.tamu.edu.

* This work was supported in part by National Science Foundation under IIS-1318638, NRI-1426752, NRI-1526200, and NRI-1748161.

(RSS) patterns. When the client cannot interrogate APs for their whereabouts and signal pattern changes, the existing WiFi localization approaches cannot handle inconsistent WiFi environments well. Their assumption of small variations in RSS spatial distribution is broken because a majority of APs may be inconsistent.

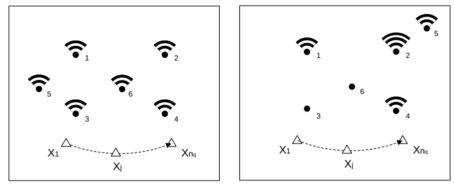

Fig. 1: Example of localization scenarios. Left: APs and their RSS readings at reference collection time. Right: APs and their RSS readings at localization time. Even though the robot's trajectory is identical, the RSS pattern may be very different which leads to unsatisfying localization results.

Building on existing WiFi fingerprinting approach, our method also employs Gaussian processes (GPs) to establish belief functions from priorly collected WiFi reference data. However, our approach utilizes two important designs to handle inconsistent APs. First, majority voting is introduced to the initial matching phase which allows us to develop a statistical hypothesis test to filter out inconsistent APs that are obvious out of places. Second, we use a windowed approach by employing a window of recent RSS readings along with relative motion information provided by inertial measurement units (IMU) to develop posterior distribution of location. We formally derive the conditional distribution and determine the length of the time window by minimizing Shannon entropy. At last, we apply the maximum likelihood estimation (MLE) method to obtain refined localization results. We have implemented our algorithm and compared it with the state of the art k-Nearest-Neighbor (k-NN) approach. The experimental results show that our method outperforms its counterpart in inconsistent WiFi environments. Specifically, our algorithm achieves a mean localization error of less than 3.7 meters when 70% of APs are inconsistent.

2 Related Work

Our work is related to the simultaneous localization and mapping (SLAM) [45] using on-board sensors. SLAM using a lidar [13] and/or a camera [4, 7, 30–32] can be more accurate but is computation intensive and suffers from reliability issues and specific requirements for environments. WiFi localization has its own advantages when considering sensor size, power, and cost. Recently, researchers have applied the graph-SLAM structure using WiFi and other wireless signals [10, 16, 34]. These methods provide good localization results, but the inconsistent WiFi environments have not been considered as SLAM in dynamic environments remains a difficult problem [21, 54]. SLAM approaches usually assume stationary environment/landmark locations. The underlying assumption that WiFi APs or RSS patterns can be treated as stationary landmarks is no longer true under inconsistent WiFi environments. In fact, inconsistent WiFi environments are highly dynamic instead of just containing a few moving landmarks in a largely stationary background.

Method	Hardware cost	Known AP Locations	Communications b/w AP and client	System/Solution
Angle based (AoA)	High	Y	Y	[11, 22, 39, 50]
Time based(ToA/ TDoA)	High	Y	Y	[12, 18, 26, 33, 46]
RSS modeling based	Low	Y	N	[1, 6, 19, 20, 27, 40, 42, 43, 48]
Fingerprint based	Low	N	N	[2, 3, 10, 14, 15, 23, 28, 35, 36, 38, 47, 49]

Table 1: Overview of WiFi Indoor Localization Methods.

WiFi localization has been a popular research area [12, 14, 29]. We can classify the existing methods into four types: angle based, time based, RSS modeling based, and fingerprinting based approaches (see Tab. 1). Angle based approaches use AP with multiple antennas to compute Angle of Arrival (AoA) of the multi-path signals received at each AP and localize through triangulation. Time based approaches include time of arrival (ToA) or time difference of arrival (TDoA) relies on the propagation time of signals traveling from a transmitter to a receiver. However, precise time synchronization is required which is not available using commodity WiFi. Both the two methods relies on known AP locations, and the client needs to interrogate APs for their locations or precise synchronization. Although more accurate in general, these two methods bear high cost in infrastructure and are difficult to be deployed. The RSS modeling based approaches model WiFi RSS signal propagation in the space assuming known AP locations, which have advantages of low cost and easy deployment. These methods often suffer from low accuracy because signal attenuation is often complex and hard to be predicted. Fingerprinting based approaches require priorly-mapped WiFi RSSs in the working space to construct a database for localization purpose which does not require communication between APs and the client or known AP locations. Our approach inherits the benefits with focus on addressing the dynamic signal pattern issues.

In order to improve WiFi localization accuracy, auxiliary sensors are combined into the above approaches, such as cameras, which are used to recognize landmarks, and IMUs for motion estimation [3, 17, 25, 37]. The sensor configuration in our approach is the same as the latter. Existing work in the IMU-assisted WiFi localization systems [8, 53] localize pedestrians by utilizing step count information to mitigate IMU drifting issue. However, the step count information is not available for robots and these methods have not explicitly consider inconsistent WiFi environments.

To deal with uncertainties in WiFi environment, existing works detect outliers using k-NN [24, 41], penalize RSS readings from uncertain APs, and signify APs with strong RSS readings in the k-NN method. Laoudias et al. [24] assume the fault model of AP with on and off status and set threshold on sum of distance of k-NN method to mitigate errors from faulty APs. These works have demonstrated the advantages of removing outliers. However, they use only RSS at the current moment which may be challenging for moving users who experience signal fluctuations. We take a windowed approach by using sequence matching which greatly improves the robustness to inconsistent APs. AP selection is not a new technique in WiFi localization. However, the main focus is to reduce the computation cost and improve accuracy instead of handling inconsistent WiFi environments. Existing approaches choose APs with the highest RSS observation [52] or select APs based on entropy-based information gain criterion [5]. They cannot be guaranteed the selected APs are reliable in inconsistent WiFi environments due to different design purposes.

3 Problem Formulation

3.1 Application Scenario and Assumptions

Our system extends the aforementioned fingerprinting methods, which assume that there is a mobile robot equipped with SLAM ability to pre-scan the environment to establish a database of WiFi RSS readings and their corresponding listening locations. The database is referred to as the WiFi reference data thereafter. It is clear that the reference data contain inconsistent AP RSSs.

At client side, the robot also perceives WiFi signal strengths and accumulates them over time which are referred to as WiFi query data. It is true that WiFi query data may also contain noisy data from inconsistent APs. The focus here is the client side localization problem in the presence of inconsistent AP signals in both query and reference data. Each localization client is equipped with an IMU. The client may be a mobile robot or a cellphone user. To focus on the most relevant issues, we have the following assumptions:

1. WiFi and IMU readings have been synchronized and time-stamped.
2. The RSS reception noises are Gaussian and IMU signal noises are white.

It is also worthing noting that we do not assume that we start with a known initial position and hence our localization is a global location problem instead of an incremental localization problem.

3.2 Notations and Problem Definition

Common notations are defined as follows,

- Reference data: $\mathbf{D} = \{(\mathbf{z}_{r,i}, X_{r,i}) | i = 1, \cdots, n\}$ is composed of n input-output pairs where i is the index variable, $X_{r,i}$ is the position in $2D$ or $3D$ Cartesian coordinate system, and vector $\mathbf{z}_{r,i}$ contains the WiFi RSS readings at $X_{r,i}$. Subscript r refers to the reference data. $\mathbf{z}_{r,i}$'s dimension is determined by number of APs in the environment. Let us define AP index $m \in M$ where $M := \{1, \cdots, m_{\max}\}$ is the AP index set. There are $m_{\max} = |M|$ distinct APs.
- Query data: subscript q refers to query data. Let j be the time index where $j \geq 0$. Vector $\mathbf{z}_{q,j}$ contains all WiFi RSS readings at time j. The sequence of WiFi query data from the beginning to time j is denoted as

$$\mathbf{z}_{q,0:j} = \{\mathbf{z}_{q,0}, \cdots, \mathbf{z}_{q,j}\}. \tag{1}$$

- IMU readings from the beginning to time j are denoted as $\mathbf{a}_{0:j}$ and $\omega_{0:j}$ for accelerations and angular velocities, respectively. Note that $\mathbf{a}_{0:j}$ and $\omega_{0:j}$ contain a lot more entries than that of query set in (1) due to high sampling frequency.

With important notations defined, let us formulate the localization problem,

Problem 1 *Given* $\mathbf{D}$*,* $\mathbf{z}_{q,0:j}$*,* $\mathbf{a}_{0:j}$*, and* $\omega_{0:j}$ *at time* j*, estimate location* X_j .

4 System Design and Algorithm

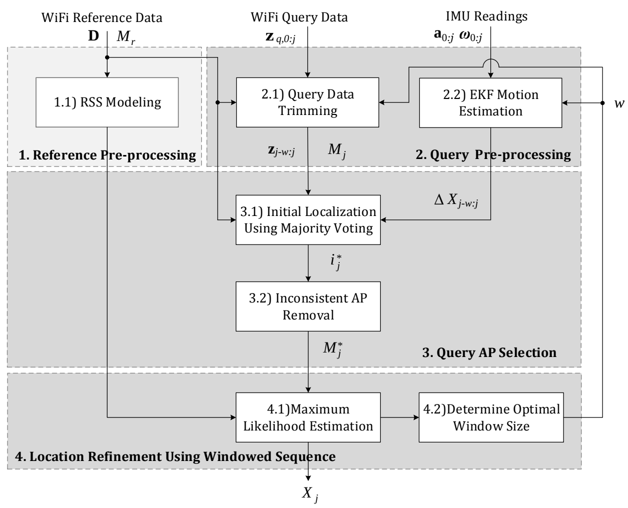

Fig. 2: System Diagram: the light gray region needs only one time computation and all the dark gray regions are computed for each frame.

Our system architecture is illustrated in Fig. 2 which contains four main blocks shaded in gray: 1) Reference pre-processing where we construct RSS-location belief model using the reference data, 2) Query pre-processing where we match a time window of query APs with reference data and reconstruct the corresponding window of relative motion of the client using IMU inputs, 3) Query AP selection where we match query WiFi with those in the reference data to remove unmatched query APs, and 4) Location estimation where we fuse the recent relative motion with historical RSS to localize the client and determine the optimal window size for next time frame. We begin with reference pre-processing (Box 1 of Fig. 2) where we construct an RSS-location belief model from the WiFi reference data using GPs.

4.1 Reference Pre-processing

Let $X_{r,i}$ be i-th location where reference data is collected and $z_{r,i,m}$ be the perceived RSS for the m-th AP at this location. $X_{r,i}$ can be either 2D or 3D depending on the environment. Let $\mathbf{X}_r := [X_{r,1}, \cdots, X_{r,n}]^\mathsf{T}$ be a location matrix containing all collection locations in the reference data $\mathbf{D}$. Define $\mathbf{z}_{r*,m} := [z_{r,1,m} \cdots, z_{r,n,m}]$ as all RSSs for the m-th AP in the reference data. Then the combined data set $\mathbf{D}_m := \{\mathbf{z}_{r*,m}, \mathbf{X}_r\}$ be the training set of the m-th AP to instantiate a GP to characterize a regression model $f_m(\cdot)$ between $\mathbf{X}_r$ and $\mathbf{z}_{r*,m}$. For each element in $\mathbf{z}_{r*,m}$,

$$z_{r,i,m} = f_m(X_{r,i}) + \varepsilon, \tag{2}$$

where $\varepsilon \sim \mathcal{N}(0, \sigma_{nm}^2)$ is the observation noise and σ_{nm}^2 is the variance. For two different locations $X_{r,i}$ and $X_{r,i'}$, we employ the kernel function $k_m(\cdot)$ in GP to characterize the correlation between their function values, namely, $f_m(X_{r,i})$ and $f_m(X_{r,i'})$:

$$k_m(X_{r,i}, X_{r,i'}) = \sigma_{fm}^2 \exp(-\frac{1}{2\lambda_m^2}|X_{r,i} - X_{r,i'}|^2), \tag{3}$$

where σ_{fm}^2 is the signal variance and λ_m is the length scale. The covariance matrix $\mathbf{K}_m$ is an $n \times n$ matrix with the (i,i')-th element $\mathbf{K}_m(i,i') = k_m(X_{r,i}, X_{r,i'})$ where $i, i' \in \{1, \cdots, n\}$. For the m-th AP, the predicted function value $\tilde{z}$ for an arbitrary location X_a conditioned on $\mathbf{X}_r$ and $\mathbf{z}_{r*,m}$ is

$$\tilde{z} = K_a^\top (\mathbf{K}_m + \sigma_{nm}^2 I)^{-1} \mathbf{z}_{r*,m}, \tag{4}$$

where I is an n-dimensional identity matrix and K_a is an $n \times 1$ vector which captures the relationship between X_a and $\mathbf{X}_r$ using (3), $K_a(i,1) = k_m(X_{r,i}, X_a)$ where $i \in \{1, \cdots, n\}$. The values of parameters σ_{fm}^2, σ_{nm}^2 and λ_m are learned using hyperparameter estimation mentioned in [10]. Since GP is a zero mean process, we subtract the mean of $\mathbf{z}_{r*,m}$ before training and add it back after to get the required $\tilde{z}$.

We can do this for each AP and hence we can obtain a location belief model based on all APs in the reference data.

4.2 Query Pre-processing

Before we match query data with the reference data, we need to remove query APs that do not exist in the reference data. It is clear that their RSSs would not assist localization. Subsequently, we reorganize $\mathbf{z}_{q,j}$ in (1) to $\mathbf{z}_j$ by trimming out the useless RSSs. Define the surviving AP index set as M_j. Similarly, we also update the historic query data set $\mathbf{z}_{0:j} := \{\mathbf{z}_0, \cdots, \mathbf{z}_j\}$ from $\mathbf{z}_{q,0:j}$. In fact, it is not necessary to employ the entire historic query data set for localization computation. We only need to backtrack a window of length w readings, which allow us to establish the windowed query data set $\mathbf{z}_{j-w:j}$ from time $j-w$ to time j. We will discuss how to determine the optimal window length in Section 4.5.

Next, we associate the relative motion from time $j-w$ to j for the query data $\mathbf{z}_{j-w:j}$. Although we do not know the absolute position, we can utilize IMU data to obtain the relative motion in the time window. We define $\Delta X_{a:b} = X_b - X_a$ as the travel distance between time a and time b. To get $\Delta X_{a:b}$, we employ an EKF-based approach for IMUs [9, 44, 51]. From the EKF, $\Delta X_{a:b}$ follows Gaussian distribution with a mean of $\overline{\Delta X_{a:b}}$ and a covariance of $\Sigma_{\Delta X_{a:b}}$. Define the relative motion set $\Delta \mathbf{X}_{j-w:j} := \{\Delta X_{j-k+1:j-k} | k = 1, \cdots, w\}$, which captures the relative motion within the time window.

4.3 Query AP Selection

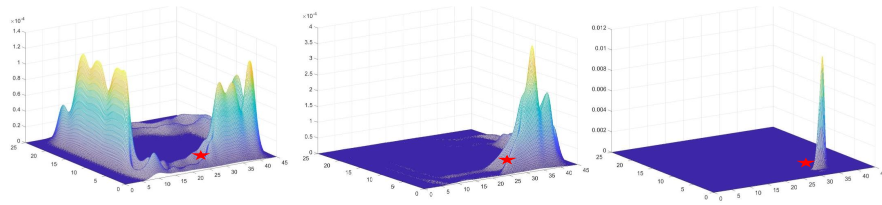

(a) (b) (c)

Fig. 3: Sample cases of posterior condition probability of robot/client location. The color changing from yellow to blue corresponds to high to low probability regions, respectively. The red star is the ground truth location. The x-axis and y-axis that span horizontal plane are 2D Cartesian coordinates, and vertical z-axis represents probability. (a) Directly computed from GPs without removing inconsistent APs and using windowed inputs. (b) After inconsistent AP removal. (c) After inconsistent AP removal and location refinement.

With $\mathbf{z}_{j-w:j}$ and $\Delta\mathbf{X}_{j-w:j}$ obtained, we can perform statistical testing to remove inconsistent APs which refers to APs that may have changed locations or have significant signal strength changes. If we do not remove inconsistent APs, localization results may suffer. In fact, we can visualize this issue. We can obtain posterior distribution of X_j directly using GPs in (4) based on $\mathbf{z}_j$ which is shown in Fig. 3(a). A desirable outcome is supposed to be a unimodal distribution with its peak close to or overlapping with the actual location. Unfortunately, the inconsistent APs have lead to a multimodal distribution and the ground truth position does not correspond to a peak position which indicated localization would fail if such belief model is naively used.

4.3.1 Initial Localization Using Majority Voting

To remove inconsistent APs, we perform an initial low resolution localization by simply assuming current location X_j is co-located at each location $X_{r,i}$ in reference set and then we can compare the sequence of RSSs. Relative motion set $\Delta\mathbf{X}_{j-w:j}$ allow us to generate assumed reference location information $\tilde{\mathbf{X}}_{r,i} = \{X_{r,i}\} \cup \{X_{r,i} - \sum_{p=1}^{k} \Delta X_{j-p:j-p+1} | k = 1, \cdots, w\}$ for the entire window. Plug $\tilde{\mathbf{X}}_{r,i}$ into (4), we obtain the assumed reference RSSs $\tilde{\mathbf{z}}_{r,i}$. Note that $\tilde{\mathbf{z}}_{r,i}$ is of the same length as $\mathbf{z}_{j-w:j}$.

Now we find the most possible location by matching query $\mathbf{z}_{j-w:j}$ to reference $\tilde{\mathbf{z}}_{r,i}$. We find best match location from initial location candidates using majority voting over best location candidates identified by each AP.

For the m-th AP at time $j-k$, its query entry in $\mathbf{z}_{j-w:j}$ is $z_{j-k,m}$ and the corresponding reference entry in $\tilde{\mathbf{z}}_{r,i}$ is $\tilde{z}_{i,m,k}$. The matching metric function f_E is the summation of the squared l^2-norm over the window,

$$f_E(m,i) = \sum_{k=0}^{w} (\tilde{z}_{i,m,k} - z_{j-k,m})^2. \tag{5}$$

The m-th AP can predict best location i_m by comparing f_E values over the entire reference set

$$i_m = \arg\min_{i \in \{1,\cdots n\}} f_E(m,i).$$

Combining the best solutions for all APs, we have a candidate solution set $I_m := \{i_m | m = 1, \cdots m_{\max}\}$. We employ majority voting to find the most agreed location index i_j^* as the solution. Specifically, we define a binary ballot function b_b:

$$b_b(i_m,i) = \begin{cases} 1, & i = i_m, \\ 0, & \text{otherwise.} \end{cases}$$

The location with the most votes wins,

$$i_j^* = \arg\max_{i \in I_m} \sum_{m=1}^{m_{\max}} b_b(i_m,i). \tag{6}$$

Now we know that the actual location is close to the location at reference index i_j^*. This information can be exploited to filter out inconsistent APs.

4.3.2 Inconsistent AP Removal

We develop statistical hypothesis testing to remove inconsistent APs. To perform the statistics testing, we begin with analyzing $f_E(m,i_j^*)$ as a distribution. We would like to derive the probability that $f_E(m,i_j^*)$ is abnormally large. For the m-th AP, have two hypotheses:

H_0 : The m-th AP is an inconsistent AP vs. H_1 : The m-th AP is a consistent AP

The significance level is α. We reject H_0 if $p-$value is less than α.

Let $\tilde{z}_{m,k}^*$ be the reference entry for the m-th AP corresponds to location i_j^*. From the GP model, we know $(\tilde{z}_{m,k}^* - z_{j-k,m})/\sigma_{nm} \sim \mathcal{N}(0,1)$ is a random variable following the normal distribution with zero mean and a variance of 1. We know that $f_E(m,i_j^*)/\sigma_{nm}^2$ is the sum of squares of multiple normal distributions according to (5), $f_E(m,i_j^*)/\sigma_{nm}^2$ has to follow χ^2-distribution with $w+1$ degrees of freedom. Its cumulative probability function is $F(x,w+1) = \dfrac{\gamma((w+1)/2,x/2)}{\Gamma((w+1)/2)}$ where $\gamma(a,x) = \int_0^x t^{a-1}e^{-t}dt$ and $\Gamma(a) = \int_0^\infty t^{a-1}e^{-t}dt$. The probability of a value from χ^2-distribution distribution is larger than x is

$$P\{f_E(m,i_j^*)/\sigma_{nm}^2 \geq x\} = 1 - F(x,w+1) = \alpha. \tag{7}$$

Setting $F(x,w+1) = 1-\alpha$ allows us to find threshold $x = F^{-1}(1-\alpha)$ where $F^{-1}(\cdot)$ is the quantile function defined as $F^{-1}(a) = inf\{y : F(y) \geq a\}$. Thus we reject H_0 if $f_E(m,i_j^*) \leq \sigma_{nm}^2 F^{-1}(1-\alpha)$. After the statistical testing, we remove inconsistent APs. The remaining AP index set is defined as M_j^*. We trim $\mathbf{z}_{j-w:j}$ accordingly. Fig. 3(b) illustrates how inconsistent AP removal help reshape the posterior location distribution which has its highest peak closer to the actual AP location. However, inconsistent AP removal cannot distinguish APs which change their positions slightly. Therefore, we still have a multi-modal distribution with many peaks, which limits the localization accuracy. To handle this issue, we introduce localization refinement.

4.4 Location Refinement Using Windowed Sequence

Our idea is to derive the posterior probability of X_j for present time j given RSS readings $\mathbf{z}_{j-w:j}$ and relative motion information $\Delta\mathbf{X}_{j-w:j}$ and then apply MLE method to obtain the location estimation (Fig. 2 Box 4).

Let $P(X_j|\mathbf{z}_{j-w:j}, \Delta\mathbf{X}_{j-w:j})$ be the posterior probability of X_j given $\mathbf{z}_{j-w:j}$ and $\Delta\mathbf{X}_{j-w:j}$. With $\Delta\mathbf{X}_{j-w:j}$, the robot/client position X_{j-k} can be obtained (see Fig. 4),

$$X_{j-k} = X_j - \Delta X_{j-k} = X_j - \sum_{p=1}^{k} \Delta X_{j-p+1:j-p}. \tag{8}$$

Assuming $X_j = x_j$, then the conditional distribution of X_{j-k} given (x_j, ΔX_{j-k}) is,

$$\mathtt{X}_{j-k}|x_j, \Delta X_{j-k} = x_j - \Delta X_{j-k}, \tag{9}$$

where operator '$\cdot|\cdot$' represents the condition for a random variable with conditions at the right side of '$|$'. Since ΔX_{j-k} is obtained from EKF based on IMU inputs, it follows Gaussian distribution with a mean of $\overline{\Delta X_{j-k}}$, and a covariance matrix of $\Sigma_{\Delta X_{j-k}}$:

$$X_{j-k}|x_j, \Delta X_{j-k} \sim \mathcal{N}(x_j - \overline{\Delta X_{j-k}}, \Sigma_{\Delta X_{j-k}}). \tag{10}$$

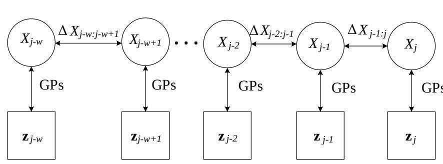

Fig. 4: Relationships between locations, displacements, and RSS readings in the window of prior locations and RSSs. Each prior location can be associated to its RSS readings using GPs.

Now let us derive the posterior probability using Bayes theorem,

$$P(X_j|\mathbf{z}_{j-w:j}, \Delta\mathbf{X}_{j-w:j}) = \frac{P(X_j, \mathbf{z}_{j-w:j}, \Delta\mathbf{X}_{j-w:j})}{P(\mathbf{z}_{j-w:j}, \Delta\mathbf{X}_{j-w:j})}. \tag{11}$$

We decompose $P(X_j, \mathbf{z}_{j-w:j}, \Delta\mathbf{X}_{j-w:j})$ by taking $\mathbf{z}_j$ to the front,

$$\begin{aligned} &P(X_j, \mathbf{z}_{j-w:j}, \Delta\mathbf{X}_{j-w:j}) \\ &= P(\mathbf{z}_j | X_j, \Delta\mathbf{X}_{j-w:j}, \mathbf{z}_{j-w:j-1}) P(X_j, \Delta\mathbf{X}_{j-w:j}, \mathbf{z}_{j-w:j-1}) \\ &= P(\mathbf{z}_j | X_j) P(X_j, \Delta\mathbf{X}_{j-w:j}, \mathbf{z}_{j-w:j-1}). \end{aligned} \tag{12}$$

This is because the current observation $\mathbf{z}_j$ only depends on the current location. Again, we decompose $P(X_j, \Delta\mathbf{X}_{j-w:j}, \mathbf{z}_{j-w:j-1})$

$$\begin{aligned} &P(X_j, \Delta\mathbf{X}_{j-w:j}, \mathbf{z}_{j-w:j-1}) \\ &= P(\mathbf{z}_{j-1} | X_j, \Delta\mathbf{X}_{j-w:j}, \mathbf{z}_{j-w:j-2}) P(X_j, \Delta\mathbf{X}_{j-w:j}, \mathbf{z}_{j-w:j-2}) \\ &= P(\mathbf{z}_{j-1} | X_{j-1} = X_j - \Delta X_{j,j-1}) P(X_j, \Delta\mathbf{X}_{j-w:j}, \mathbf{z}_{j-w:j-2}). \end{aligned} \tag{13}$$

This is because $\mathbf{z}_{j-1}$ is independent of $\mathbf{z}_{j-w;j-2}$ given X_{j-1}.
For $P(X_j, \Delta\mathbf{X}_{j-w:j}, \mathbf{z}_{j-w:j-2})$, we have

$$\begin{aligned} &P(X_j, \Delta\mathbf{X}_{j-w:j}, \mathbf{z}_{j-w:j-2}) \\ &= P(\mathbf{z}_{j-2} | X_j, \Delta\mathbf{X}_{j-w:j}, \mathbf{z}_{j-w:j-3}) P(X_j, \Delta\mathbf{X}_{j-w:j}, \mathbf{z}_{j-w:j-3}) \\ &= P(\mathbf{z}_{j-2} | X_{j-2} = X_j - \sum_{p=1}^{2} \Delta X_{j-p+1,j-p}) P(X_j, \Delta\mathbf{X}_{j-w:j}, \mathbf{z}_{j-w:j-3}). \end{aligned} \tag{14}$$

X_{j-2} and X_j are related using (8). By decomposing $P(X_j | \mathbf{z}_{j-w:j}, \Delta\mathbf{X}_{j-w:j})$ iteratively, we rewrite (11) as

$$P(X_j | \mathbf{z}_{j-w:j}, \Delta\mathbf{X}_{j-w:j}) = \frac{P(\mathbf{z}_j | X_j) \prod_{k=1}^{w} P(\mathbf{z}_{j-k} | X_{j-k} = X_j - \sum_{p=1}^{k} \Delta X_{j-p+1,j-p})}{P(\mathbf{z}_{j-w:j}, \Delta\mathbf{X}_{j-w:j})}. \tag{15}$$

We integrate displacement $\Delta\mathbf{X}_{j-k:j}$ for each term:

$$P(\mathbf{z}_{j-k} | X_{j-k} = X_j - \sum_{p=1}^{k} \Delta X_{j-p+1,j-p}) = \int P(\mathbf{z}_{j-k} | x_{j-k}) f(\Delta x_{j-k}) d(\Delta x_{j-k}), \tag{16}$$

where $f(\Delta x_{j-k})$ is a Gaussian distribution function (10) obtained from EKF result.

Under the GP model, the probability distribution for the m-th AP's RSS conditioned on $X_j = x_j$ is

$$z_{j,m} | X_j \sim \mathcal{N}(\mu_m(x_j, \mathbf{D}), \Sigma_m(x_j, \mathbf{D})), \tag{17}$$

where $\mu_m(x_j, \mathbf{D}) = k_{X_j}^T (K_m + \sigma_{nm}^2 I)^{-1} \mathbf{z}_{r,*m}^T$ and $\Sigma_m(x_j, \mathbf{D}) = k(x_j, x_j) - k_{X_j}^T (K_m + \sigma_{nm}^2 I)^{-1} k_{X_j}$ with $k(x_j, x_j) = \sigma_{fm}^2$ obtained from (3). Since RSSs of all APs are independent, we have

$$f(\mathbf{z}_j | X_j = x_j) = \prod_{m \in M_j^*} f(z_{j,m} | X_j = x_j). \tag{18}$$

Similarly, we can obtain a probability distribution function for $\mathbf{z}_{j-k}|X_{j-k}$. With results from (16) and (18) and the fact that $\mathbf{z}_{j-w:j}$ and $\Delta\mathbf{X}_{j-w:j}$ are independent, we can compute (15) to obtain $P(X_j|\mathbf{z}_{j-w:j}, \Delta\mathbf{X}_{j-w:j})$. Fig. 3(c) illustrates the posterior distribution for the windowed inputs which appears as a unimodal distribution with its peak located close to the actual location. This significantly increases the accuracy of the localization algorithm.

Finally, we estimate X_j by applying MLE to the posterior probability in (15),

$$\hat{X}_j = \arg\max_{X_j} P(\mathbf{z}_j|X_j) \int \prod_{k=1}^{w} P(\mathbf{z}_{j-k}|X_{j-k} = X_j - \sum_{p=1}^{k} \Delta X_{j-p+1,j-p}) d(\Delta x_{j-k}). \tag{19}$$

Note that we dropped the denominator in (15) because it is not a function of X_j.

4.5 Determine Optimal Window Size

The remaining issue is how to determine the optimal window size w of RSS sequence. It is worth noting that increasing window size w significantly increases computation load. Also, the relative motion information $\Delta\mathbf{X}_{j-w:j}$ has its variance increasing over time due to IMU drifting and eventually becomes useless due to its large spatial uncertainty. To choose an appropriate window size, we minimize the Shannon entropy over window size. Define A as a latticed set of the localization space. The lattice resolution is 0.1 meters in each dimension in our settings. Define $H(w, j)$ as the Shannon entropy over the probability distribution $P(X_j|\mathbf{z}_{j-w:j}, \Delta\mathbf{X}_{j-w:j})$,

$$H(w, j) = -\sum_{X_j \in A} P(X_j|\mathbf{z}_{j-w:j}, \Delta\mathbf{X}_{j-w:j}) \log P(X_j|\mathbf{z}_{j-w:j}, \Delta\mathbf{X}_{j-w:j}).$$

We choose the optimal w that minimizes $H(w, j)$ over all possible window length set $\mathbf{w} := \{0, 1, ..., w_{\max}\}$ where $w_{\max}$ is the maximum allowable window size that covers the entire A. Then we find the optimal solution w^*,

$$w^* = \arg\min_{w \in \mathbf{w}} H(w, j). \tag{20}$$

The resulting w^* will be used as the window size for time frame $j+1$.

5 Experiments

We have implemented our algorithm using MATLAB under a PC with Windows 7. We evaluate our method using real world data from physical experiments. Three algorithms are compared in our experiment.

Building	HRBB	SCTS	WEB
Trajectory (meters)	96	50	80
Reference Data # of AP	252	132	159
Query Data AP # of AP	246	135	171
Shared APs between two data sets	195	130	158

Table 2: Dataset Description

		Inconsistent APs									
Dataset	Method	0%	10%	20%	30%	40%	50%	60%	70%	80%	90%
HRBB	*k*-NN	3.3	3.5	3.8	4.2	4.4	5.5	6.5	8.6	9.7	15.1
	MLE-NS	**3.2**	3.4	3.9	4.2	4.3	5.6	7.0	6.7	7.3	10.0
	MLE-S	**3.2**	**3.2**	**3.2**	**3.2**	**3.2**	**3.2**	**3.2**	**3.5**	**4.6**	**9.1**
SCTC	*k*-NN	**1.6**	1.8	1.9	2.6	3.0	3.8	5.8	7.1	8.0	10.4
	MLE-NS	2.1	2.1	2.1	2.6	2.9	3.6	6.9	6.6	6.4	**6.4**
	MLE-S	1.7	**1.6**	**1.7**	**1.7**	**2.1**	**2.0**	**2.4**	**3.1**	**4.9**	10.1
WSB	*k*-NN	**1.2**	**1.3**	**1.3**	1.5	2.1	2.9	6.2	8.9	12.7	16.3
	MLE-NS	1.6	1.5	1.6	1.7	1.9	2.3	4.4	6.4	**8.9**	**14.5**
	MLE-S	1.4	1.5	1.4	**1.4**	**1.4**	**1.6**	**2.3**	**3.7**	10.3	19.4

Table 3: Mean Localization Error (meters)

- MLE-S: Our complete method including both AP removal and MLE refinement,
- MLE-NS: our algorithm without AP removal in Section 4.3.2. We test this variant of our method to show the benefit of inconsistent AP removal, and
- *k*-NN [17]: This method is chosen as the counterpart because it has ability to handle some degrees of inconsistent WiFi environments despite it only targets at handling RSS fluctuations. It also employs IMU to assist WiFi localization. For brevity, we name it as *k*-NN method here.

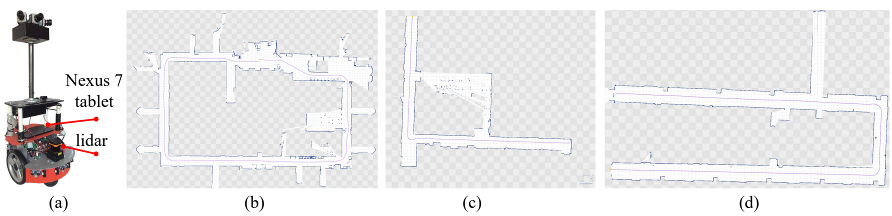

Fig. 5: (a) Our data collection robot and sensor configuration. 2D lidar maps are used as ground truth: (b) HRBB, (c) SCTS, and (d) WEB.

Dataset: We have collected datasets from three different buildings: H. R. Bright building (HRBB), Scoates Hall (SCTS), and Wisenbaker Engineering Building (WEB) at Texas A&M University using a Nexus 7 tablet and a mobile robot (see Fig. 5). Our robot is equipped with a Hokuyo UTM-30LX lidar and provides 2D lidar map (see Fig. 5 (b)) with timestamps. The location from lidar-based SLAM is used as a ground truth with an error of less than 10 centimeters. The dataset consists of WiFi RSS readings collected at 1Hz and IMU readings at 100Hz. Tab. 2 describes details of each dataset including the overall trajectory, the number of APs in reference data, and query data. We have collected the reference data and query data in different days. Therefore, the two data sets do not share the exact same number of APs. The shared AP number are shown in the last row of the Tab. 2.

Evaluation Metric: The localization error at time j is defined as the Euclidean distance between the estimation $\hat{X}_j$ and ground truth $X_{g,j}$: $\varepsilon_j = ||\hat{X}_j - X_{g,j}||$. The error is measured in meters.

Tab. 3 shown the test results. The best results are highlighted in bold fonts. We have tested all three algorithms under different percentage of inconsistent APs ranging from 0% to 90% in the environment. To generate inconsistent APs, we first use systematic random sampling on the shared APs between reference data and query data and shift AP RSS patterns randomly to form inconsistent APs. It is clear that our method is more robust than the counterpart under inconsistent WiFi environments. Also, the inconsistent AP removal process does help in maintain consistent localization accuracy up to 70% inconsistent APs. Our methods achieve the best or close to the best mean localization error as long as the inconsistent AP ratio is less than 70%. At 80% or 90% inconsistent AP ratio, our proposed method does not work well, this is because signal to noise ratio is too low and inconsistent AP removal process may fail.

Fig. 6 shows the effectiveness of inconsistent AP removal scheme by illustrating true positive (TP) rates, which is defined as

$$TP = \frac{\#\text{consistent AP selected}}{\#\text{All selected APs}},$$

over different inconsistent AP ratios. Our method ensures that TP rates remain above 0.5 under 70% inconsistent APs environment among different datasets with a mean localization error less than 3.7 meters.

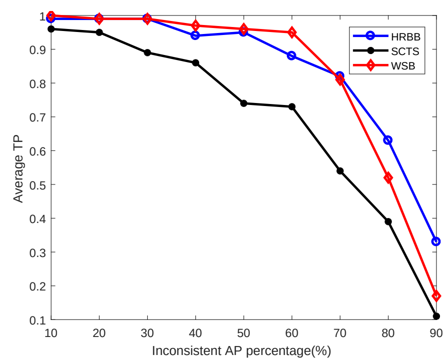

Fig. 6: Average TP rates of selected APs after the AP removal process.

The last evaluation is runtime of our approach. From We report the average runtime for each time frame are 0.30 seconds on average for SCTS dataset, 0.89 seconds for HRBB dataset, and 0.63 seconds for WEB dataset. From alogithm analysis, the most time consuming operation is computing location posterior probability which is proportional to the number of APs (Tab. 2.). Our runtime result confirm it. Recall that the time interval for each time frame is 1 second in experiment set up, the runtime for localization is tolerable.

6 Conclusion and Future Work

We reported a WiFi-based localization method designed to handle inconsistent WiFi environments where mobile APs and APs with beamforming capabilities cause significant changes in radiation patterns in RSSs. Building on the WiFi fingerpinting method that utilizes GPs to establish a belief model from reference data, our method employed majority voting along with embedded statistical hypothesis testing to remove inconsistent APs. Instead of using RSS pattern at a single time instance, we used a historical sequence to further improve the robustness to inconsistent APs. We derived a posterior location distribution function for the sequence and applied MLE to refine localization results. Our method was tested and compared to an existing method. The results showed that our method outperforms the counterpart and our design is effective. In the future, we will conduct more experiments and comparison studies. We will also focus on analysis and improving computation speed.

Acknowledgment

We would like to thank C. Chou, B. Li, S. Yeh, A. Kingery, A. Angert, Y. Sun, M. Jin, D. Wang, Y. You, M. Momin, T. Sun, and H. Li for their input and contributions to the NetBot Lab at Texas A&M University.

References

1. P. Bahl and V. N. Padmanabhan. RADAR: an in-building RF-based user location and tracking system. In *Proceedings of the IEEE international Conference on Computer Communications(INFOCOM), Tel-Aviv, Israel*, Mar. 2000.
2. Benjamin Balaguer, Gorkem Erinc, and Stefano Carpin. Combining classification and regression for wifi localization of heterogeneous robot teams in unknown environments. In *The 2012 IEEE/RSJ International Conference on Intelligent Robots and Systems (IROS)*, 2012.
3. J. Biswas and M. Veloso. WiFi localization and navigation for autonomous indoor mobile robots. In *IEEE International Conference on Robotics and Automation (ICRA), Anchorage, USA*, May 2010.
4. Nicholas Carlevaris-Bianco and Ryan M Eustice. Learning visual feature descriptors for dynamic lighting conditions. In *IEEE/RSJ International Conference on Intelligent Robots and Systems (IROS)*, pages 2769–2776, 2014.
5. Yiqiang Chen, Qiang Yang, Jie Yin, and Xiaoyong Chai. Power-efficient access-point selection for indoor location estimation. *IEEE Transactions on Knowledge and Data Engineering*, 18(7):877–888, July 2006.
6. Krishna Chintalapudi, Anand Padmanabha Iyer, and Venkata N. Padmanabhan. Indoor localization without the pain. In *Proceedings of the Sixteenth Annual International Conference on Mobile Computing and Networking (MobiCom)*, 2010.
7. Javier Civera, Oscar G Grasa, Andrew J Davison, and JMM Montiel. 1-point RANSAC for extended Kalman filtering: Application to real-time structure from motion and visual odometry. *Journal of Field Robotics*, 27(5):609–631, 2010.
8. Zhi-An Deng, Ying Hu, Jianguo Yu, and Zhenyu Na. Extended kalman filter for real time indoor localization by fusing wifi and smartphone inertial sensors. *Micromachines*, 6(4):523–543, 2015.
9. G. Dissanayake, S. Sukkarieh, E. Nebot, and H. Durrant-Whyte. The aiding of a low-cost strapdown inertial measurement unit using vehicle model constraints for land vehicle applications. *IEEE Transactions on Robotics and Automation*, 17(5):731–747, Oct 2001.
10. Brian Ferris, Dieter Fox, and Neil Lawrence. WiFi-SLAM using gaussian process latent variable models. In *Proceedings of the 20th International Joint Conference on Artifical Intelligence, Hyderabad, India*, Jan. 2007.
11. Jon Gjengset, Jie Xiong, Graeme McPhillips, and Kyle Jamieson. Phaser: Enabling phased array signal processing on commodity wifi access points. In *Proceedings of the 20th annual international conference on Mobile computing and networking*, pages 153–164. ACM, 2014.
12. Ismail Guvenc and Chia-Chin Chong. A survey on toa based wireless localization and nlos mitigation techniques. *IEEE Communications Surveys & Tutorials*, 11(3), 2009.
13. Dirk Hahnel, Wolfram Burgard, Dieter Fox, and Sebastian Thrun. An efficient FastSLAM algorithm for generating maps of large-scale cyclic environments from raw laser range mea-

surements. In *IEEE/RSJ International Conference on Intelligent Robots and Systems (IROS)*, volume 1, pages 206–211, 2003.
14. S. He and S. H. G. Chan. Wi-fi fingerprint-based indoor positioning: Recent advances and comparisons. *IEEE Communications Surveys Tutorials*, 18(1):466–490, 2016.
15. Andrew Howard, Sajid Siddiqi, and Gaurav S Sukhatme. An experimental study of localization using wireless ethernet. In *Field and Service Robotics*, pages 145–153. Springer, 2003.
16. J. Huang, D. Millman, M. Quigley, D. Stavens, S. Thrun, and A. Aggarwal. Efficient, generalized indoor wifi graphslam. In *IEEE International Conference on Robotics and Automation (ICRA), Shanghai, China*, pages 1038–1043, May 2011.
17. M. Jin, B. Koo, S. Lee, C. Park, M. J. Lee, and S. Kim. IMU-assisted nearest neighbor selection for real-time WiFi fingerprinting positioning. In *International Conference onIndoor Positioning and Indoor Navigation (IPIN), Zurich, Switzerland*, Oct 2014.
18. Kiran Raj Joshi, Steven Siying Hong, and Sachin Katti. Pinpoint: Localizing interfering radios. In *NSDI*. USENIX, 2013.
19. C. Kim, D. Song, Y. Xu, J. Yi, and X. Wu. Cooperative search of multiple unknown transient radio sources using multiple paired mobile robots. *IEEE Transactions on Robotics*, 30(5):1161–1173, Oct. 2014.
20. C. Kim, D. Song, J. Yi, and X. Wu. Decentralized searching of multiple unknown and transient radio sources with paired robots. *Engineering*, 1(1):58 – 65, July 2015.
21. D. H. Kim and J. H. Kim. Effective background model-based rgb-d dense visual odometry in a dynamic environment. *IEEE Transactions on Robotics*, 32(6):1565–1573, Dec 2016.
22. Manikanta Kotaru, Kiran Joshi, Dinesh Bharadia, and Sachin Katti. Spotfi: Decimeter level localization using wifi. *SIGCOMM Comput. Commun. Rev.*, 45(4):269–282, Aug 2015.
23. Andrew M Ladd, Kostas E Bekris, Algis Rudys, Lydia E Kavraki, and Dan S Wallach. Robotics-based location sensing using wireless ethernet. *Wireless Networks*, 11(1-2):189–204, 2005.
24. Christos Laoudias, Michalis P Michaelides, and Christos G Panayiotou. Fault detection and mitigation in wlan rss fingerprint-based positioning. *Journal of Location Based Services*, 6(2):101–116, 2012.
25. W. W. L. Li, R. A. Iltis, and M. Z. Win. A smartphone localization algorithm using rssi and inertial sensor measurement fusion. In *2013 IEEE Global Communications Conference (GLOBECOM)*, Dec 2013.
26. Xinrong Li and Kaveh Pahlavan. Super-resolution toa estimation with diversity for indoor geolocation. *IEEE Transactions on Wireless Communications*, 3(1):224–234, 2004.
27. Hyuk Lim, Lu-Chuan Kung, Jennifer C. Hou, and Haiyun Luo. Zero-configuration indoor localization over ieee 802.11 wireless infrastructure. *Wirel. Netw.*, 16(2), FEB. 2010.
28. Hongbo Liu, Yu Gan, Jie Yang, Simon Sidhom, Yan Wang, Yingying Chen, and Fan Ye. Push the limit of wifi based localization for smartphones. In *Proceedings of the 18th Annual International Conference on Mobile Computing and Networking (MobiCom)*, 2012.
29. Hui Liu, Houshang Darabi, Pat Banerjee, and Jing Liu. Survey of wireless indoor positioning techniques and systems. *IEEE Transactions on Systems, Man, and Cybernetics, Part C (Applications and Reviews)*, 37(6):1067–1080, 2007.
30. Y. Lu and D. Song. Visual navigation using heterogeneous landmarks and unsupervised geometric constraints. In *IEEE Transactions on Robotics (T-RO)*, volume 31, pages 736 – 749, June 2015.
31. Yan Lu and Dezhen Song. Robust RGB-D odometry using point and line features. In *IEEE International Conference on Computer Vision (ICCV), Santiago, Chile*, Dec. 2015.
32. András Majdik, Dorian Gálvez-López, Gheorghe Lazea, and José A Castellanos. Adaptive appearance based loop-closing in heterogeneous environments. In *IEEE/RSJ International Conference on Intelligent Robots and Systems (IROS)*, pages 1256–1263, 2011.
33. Alex T Mariakakis, Souvik Sen, Jeongkeun Lee, and Kyu-Han Kim. Sail: Single access point-based indoor localization. In *Proceedings of the 12th annual international conference on Mobile systems, applications, and services*, pages 315–328. ACM, 2014.

34. P. Mirowski, T. K. Ho, Saehoon Yi, and M. MacDonald. Signalslam: Simultaneous localization and mapping with mixed wifi, bluetooth, lte and magnetic signals. In *International Conference on Indoor Positioning and Indoor Navigation*, pages 1–10, Oct 2013.
35. Rajalakshmi Nandakumar, Krishna Kant Chintalapudi, and Venkata N. Padmanabhan. Centaur: Locating devices in an office environment. In *Proceedings of the 18th Annual International Conference on Mobile Computing and Networking*, 2012.
36. M Ocana, LM Bergasa, MA Sotelo, J Nuevo, and R Flores. Indoor robot localization system using wifi signal measure and minimizing calibration effort. In *Proceedings of the IEEE International Symposium on Industrial Electronics, Dubrovnik, Croatia*, June 2005.
37. M. Quigley, D. Stavens, A. Coates, and S. Thrun. Sub-meter indoor localization in unmodified environments with inexpensive sensors. In *The 2010 IEEE/RSJ International Conference on Intelligent Robots and Systems (IROS), Taipei, Taiwan*, Oct 2010.
38. S. Saha, K. Chaudhuri, D. Sanghi, and P. Bhagwat. Location determination of a mobile device using IEEE 802.11b access point signals. In *IEEE Wireless Communications and Networking Conference(WCNC), New Orleans, LA, 2003*, March 2003.
39. Souvik Sen, Jeongkeun Lee, Kyu-Han Kim, and Paul Congdon. Avoiding multipath to revive inbuilding wifi localization. In *Proceeding of the 11th Annual International Conference on Mobile Systems, Applications, and Services*, MobiSys '13. ACM, 2013.
40. Oscar Serrano, José Marıa Canas, Vicente Matellán, and Luis Rodero. Robot localization using WiFi signal without intensity map. In *International Workshop on Algorithmic Foundationsof Robotics (WAFR), Utrecht/Zeist, The Netherlands*, July 2004.
41. Jungmin So, Joo-Yub Lee, Cheal-Hwan Yoon, and Hyunjae Park. An improved location estimation method for wifi fingerprint-based indoor localization. *International Journal of Software Engineering and Its Applications*, 7(3):77–86, 2013.
42. D. Song, C. Kim, and J. Yi. Simultaneous localization of multiple unknown CSMA-based wireless sensor network nodes using a mobile robot with a directional antenna. *Journal of Intelligent Service Robots*, 2(4):219–233, Oct. 2009.
43. D. Song, C. Kim, and J. Yi. Simultaneous localization of multiple unknown and transient radio sources using a mobile robot. *IEEE Transactions on Robotics*, 28(3):668–680, June 2012.
44. Salah Sukkarieh, Peter Gibbens, Ben Grocholsky, Keith Willis, and Hugh F Durrant-Whyte. A low-cost, redundant inertial measurement unit for unmanned air vehicles. *The International Journal of Robotics Research*, 19(11):1089–1103, June 2000.
45. Sebastian Thrun, Wolfram Burgard, and Dieter Fox. *Probabilistic Robotics*. MIT Press, 2005.
46. Deepak Vasisht, Swarun Kumar, and Dina Katabi. Decimeter-level localization with a single wifi access point. In *NSDI*, 2016.
47. He Wang, Souvik Sen, Ahmed Elgohary, Moustafa Farid, Moustafa Youssef, and Romit Roy Choudhury. No need to war-drive: Unsupervised indoor localization. In *Proceedings of the 10th International Conference on Mobile Systems, Applications, and Services*, MobiSys '12, 2012.
48. Kamin Whitehouse, Chris Karlof, and David Culler. A practical evaluation of radio signal strength for ranging-based localization. *SIGMOBILE Mob. Comput. Commun. Rev.*, 11(1), January 2007.
49. C. Wu, Z. Yang, and Y. Liu. Smartphones based crowdsourcing for indoor localization. *IEEE Transactions on Mobile Computing*, 14(2):444–457, Feb 2015.
50. Jie Xiong and Kyle Jamieson. Arraytrack: A fine-grained indoor location system. In *(NSDI)*, pages 71–84. USENIX, 2013.
51. J. Yi, H. Wang, J. Zhang, D. Song, S. Jayasuriya, and J. Liu. Modeling and analysis of skid-steered mobile robots with applications to low-cost inertial measurement unit-based motion estimation. *IEEE Transactions on Robotics*, 25(5):1087–1097, Oct. 2009.
52. M. A. Youssef, A. Agrawala, and A. Udaya Shankar. Wlan location determination via clustering and probability distributions. In *Proceedings of the First IEEE International Conference on Pervasive Computing and Communications, 2003. (PerCom 2003).*, March 2003.
53. Y. Zhuang and N. El-Sheimy. Tightly-coupled integration of wifi and mems sensors on handheld devices for indoor pedestrian navigation. *IEEE Sensors Journal*, 16(1):224–234, 2016.
54. D. Zou and P. Tan. Coslam: Collaborative visual slam in dynamic environments. *IEEE Transactions on Pattern Analysis and Machine Intelligence*, 35(2):354–366, Feb 2013.